Highly Spin-Polarized, Nearly Free-Electron States in Front of Co($10\bar{1}0$)

Sven Bode,[1] Kai Starke,[1] Peter Rech,[2] and Günter Kaindl[1]
[1]*Institut für Experimentalphysik, Freie Universität Berlin, Arnimallee 14, D-14195 Berlin-Dahlem, Germany*
[2]*Institut für Physikalische Chemie, Freie Universität Berlin, Takustrasse 3, D-14195 Berlin-Dahlem, Germany*
(Received 21 October 1993)

We report on the first observation of highly spin-polarized nearly free-electron image-potential states. At the surface Brillouin zone boundary $\overline{Y}$ of Co($10\bar{1}0$) spin-polarized inverse photoemission reveals large exchange splittings of 125 meV and 96 meV for two $n = 1$ image states, separated by 0.6 eV due to the surface corrugation potential. The exchange splittings are nearly as large as the intrinsic linewidths so that electrons trapped in these two-dimensional states are highly spin polarized. By their large exchange splitting these image states serve as a test case for a possible spin dependence of the surface-barrier potential.

PACS numbers: 73.20.-r, 75.30.Pd, 79.60.Bm

The spin dependence of electronic surface states on ferromagnetic metals is of particular interest in surface magnetism: It serves as an indicator of the magnetic properties of the outermost atomic layer. Free-electron-like surface states reside in Shockley-inverted gaps of the bulk band structure and one conveniently distinguishes crystal induced states from image potential states [1]. The probability distributions of crystal-induced states have their maximum within the surface layer and on Ni surfaces their exchange splitting is nearly as large as the splitting of the *sp*-like bulk bands at the edges of the corresponding gaps [2,3]. The $\frac{1}{4z}$ dependence of the image potential leads to a Rydberg-like series of states spanning about 1 eV below the vacuum energy E_V [4]; in these states, electrons are trapped between surface barrier potential and outermost layer [1,5]. In contrast to crystal-induced states, the wave functions of image states peak a few Å in front of the crystal, thus having little overlap with the bulk bands. Therefore, image states are expected to exhibit much smaller exchange splittings than crystal-induced states. Reliable experimental information on the spin dependence of image states at clean ferromagnetic surfaces has been obtained recently by spin-polarized inverse photoemission (IPE) from Ni. On Ni(001) an exchange splitting of 13 ± 13 meV was observed for the lowest Rydberg state ($n = 1$) at $\overline{\Gamma}$, the center of the surface Brillouin zone (SBZ) [3], and at Ni(111)$\overline{\Gamma}$ a splitting of 18 ± 3 meV is measured [6]. Thus on Ni surfaces the splitting of image states is much smaller than their intrinsic linewidth [e.g., 84 meV at Ni(111) as observed by non-spin-resolved two-photon photoelectron spectroscopy [7]]. The image-state splitting is explained to result mainly from a nonvanishing exchange splitting of bulk bands at the boundaries which confine the gap [8], yet the gap-boundary splittings do not exceed ≈ 0.2 eV in case of Ni [3]. For Fe and Co surfaces, by contrast, much larger image-state splittings can be expected due to the large bulk *d*-band exchange splittings of up to 2.1 eV and 1.2 eV, respectively [9,10]. However, up to now there have been no spin-polarized IPE studies either on Fe or on Co surfaces, except for an early investigation of Fe(110)$\overline{\Gamma}$ with a longitudinally polarized electron beam unable to reveal magnetic information at $\overline{\Gamma}$ [11]. From experiment there exists only an upper bound of ≈ 0.1 eV for the image-state splitting at Fe(110)$\overline{\Gamma}$ and Co(0001)$\overline{\Gamma}$ estimated from non-spin-polarized IPE data [12].

For the ($10\bar{1}0$) surface of hcp Co a large Shockley-inverted bulk band gap extending from ≈ 2 eV to ≈ 8 eV above the Fermi energy E_F is expected theoretically at the SBZ boundary $\overline{Y}$ [13]. These linear muffin-tin orbital calculations predict a large exchange splitting for the upper (0.96 eV) as well as for the lower gap edge (0.67 eV) at $\overline{Y}$, due to considerable *sd* hybridization at the *L* points which confine the gap. In addition, the effective vacuum energy at $\overline{Y}$ lies well inside the gap, i.e., in the region of high surface reflectivity. The Co($10\bar{1}0$) $\overline{Y}$ gap thus serves as an ideal test case for studying the spin dependence of image states in a strongly exchange-split bulk band gap at the SBZ boundary.

In this Letter we report on the first observation of image-state exchange splittings on Co($10\bar{1}0$) which are nearly 1 order of magnitude larger than those so far observed on clean ferromagnetic surfaces. At the SBZ boundary $\overline{Y}$ spin-polarized IPE reveals two $n = 1$ Rydberg states, separated by 0.6 eV due to an effective corrugation of the crystal potential sensed a few Å in front of the surface layer. The exchange splittings of 125 meV and 96 meV are shown to be comparable with the intrinsic linewidths so that electrons trapped in these two-dimensional nearly free-electron states are highly spin polarized.

The IPE measurements were performed with a longitudinally spin-polarized electron source with a spin polarization of $P = 30 \pm 3\%$. The angle of electron incidence was varied in the ΓALM mirror plane of the Co sample by rotating the sample holder. Photons emitted from the sample are detected by a SrF_2-iodine-bandpass counter ($\hbar\omega = 9.4 \pm 0.2$ eV). In the present case of image-state spectra at Co($10\bar{1}0$)$\overline{Y}$ the counter is placed at 60° relative to the surface normal. Such a large angle allows

0031-9007/94/72(7)/1072(4)$06.00

an efficient detection of light from dipole transitions into *sp*-like surface states which is polarized along the surface normal [14]. Further details of the spin-polarized IPE apparatus are described elsewhere [15].

The in-plane magnetized Co(10$\bar{1}$0) crystal ($10 \times 5 \times 1\,\mathrm{mm}^3$) is held in a soft iron yoke to achieve closed flux geometry; this yields a high remanent magnetization and minimizes stray fields from the sample [3]. In contrast to cubic Fe and Ni, hcp Co is a uniaxial ferromagnet in which no flux can be transported normal to the c axis (easy axis); thus no flux closure can be achieved in a Co picture-frame crystal. All spectra were obtained from the remanently magnetized sample since a defined momentum in IPE is not compatible with application of external fields during measurement. Remanent magnetization was achieved by short current pulses ($\approx$ 140 A, $\approx$ 1 ms) applied through a self-supporting noninsulated solenoid (10 turns) wound around the yoke. The magnetization was measured *in situ* by UHV compatible magneto-optical Kerr effect (MOKE) [16]. The MOKE data revealed small oppositely magnetized stripe domains at remanence covering $\approx$8% of the surface; this corresponds to a reduced average surface magnetization $\mathbf{J} \approx 84\,\mathbf{J_s}$ of the saturation magnetization at room temperature. Since the size of the experimental spin asymmetry depends only on the inner product $\mathbf{P}\cdot\mathbf{J}$ the reduced average magnetization manifests itself in the experimental asymmetry in exactly the same way as a reduced beam polarization P [17]. All spin-polarized IPE spectra are normalized to the hypothetical case of a saturated (single domain) surface *and* a 100% polarized electron beam. Reliable values for the spin splittings were obtained in the following way: "True" spin effects remain unaffected upon simultaneous reversal of both vectors, **P** and **J**, but change sign upon reversal of only one vector. Therefore, a series of spectra was recorded for each of the four combinations of vector orientations; the spin asymmetries of these spectra were—except for the sign—identical.

The Co(10$\bar{1}$0) surface was cleaned by about 100 cycles of sputtering with 0.5 kV Ne ions (6 μA, 4 min, room temperature) and annealing to 650 K (for 25 min) until no traces of contaminants (N,C,O,...) were observed by Auger emission spectroscopy (sensitivity $\approx$ 1% of atomic layer). Residual C contamination beyond AES sensitivity was removed by chemical titration with 0.02 L O_2 at T = 600 K; surplus oxygen in turn was removed by 2 L H_2. During this final procedure the IPE intensity of crystal-induced and image-potential states at $\bar{Y}$ was used to monitor surface cleanliness. All IPE spectra were recorded at room temperature.

Spin-integrated IPE spectra of Co(10$\bar{1}$0)$\bar{Y}$ are shown in Fig. 1. Above the Co d bands (a), four spectral features are clearly discernible inside the exchange-split gap (white area). The two states near the lower gap edges (b) are assigned as a spin pair of crystal-induced surface states; an exchange splitting of 0.7 eV is obtained from

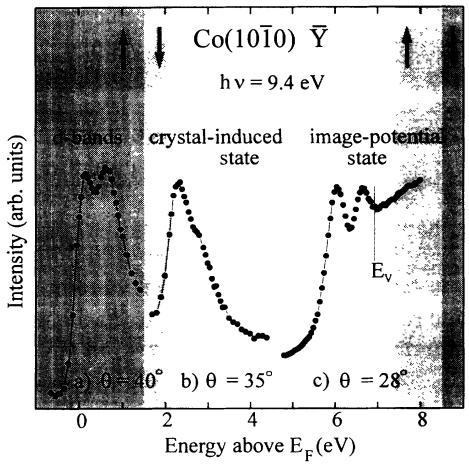

FIG. 1. Spin-integrated IPE spectra of (a) the d-band, (b) the crystal-induced, and (c) the image-potential surface states on Co(10$\bar{1}$0) near the SBZ boundary $\bar{Y}$. The spectra were taken at three different angles of electron incidence: (a) Θ = 40°, (b) Θ = 35°, and (c) Θ = 28° relative to the surface normal. The energy range of the spin-dependent bulk band structure (from Ref. [13]) is indicated by shaded areas. E_V denotes the effective vacuum energy at $\bar{Y}$ $E_V = \Phi + \hbar^2 k_{||}^2/2m = 6.72$ eV with $\Phi = 4.45$ eV.

the corresponding spin-resolved spectra [18]. The two states which appear within 1 eV below E_V are identified as image states, namely, the lowest members of the odd ($n = 1^-$) and even ($n = 1^+$) Rydberg series. Such a doubling of surface states near the SBZ boundary has been observed before in the case of crystal-induced states at Cu(110)$\bar{Y}$ [19] and Ni(110)$\bar{Y}$ [20]. It is due to the corrugation of the potential felt by electrons moving parallel to the surface. The corrugation energetically separates surface states with wave functions of maximum probability *at* the surface atoms (s-like) and those with maximum probability *between* atoms (p-like) [5].

An analogous symmetry splitting is theoretically expected for image-potential states [21]. Yet, such a pair of image states could not be found experimentally on the fcc (110) surfaces since the effective vacuum energy E_V at $\bar{Y}$ exceeds by far the upper gap edges. In the present situation, however, E_V lies well inside the gap. The energy difference of 0.6 eV between the $n = 1^-$ and the $n = 1^+$ states can be regarded as a measure of the effective corrugation "$2V_G^{\mathrm{surf}}$" of the crystal potential sensed by electrons captured a few Å in front of the surface. Hereby, for the first time, it is experimentally demonstrated that surface corrugation considerably influences the dispersion behavior of an image state. Previous attempts to relate large effective masses of image states (in $\bar{\Gamma}$ gaps) with surface corrugation have failed [5]. Note that the energy difference between the two peaks would not conflict with an assignment of the upper peak as $n = 2^-$. However, this is very unlikely for two reasons: (1) Even in gaps at

$\overline{\Gamma}$ no $n = 2$ state is uniquely discernible on Ni and Cu surfaces despite a good signal-to-background ratio for the $n = 1$ peaks [3,6,22]. (2) $n = 2$ wave functions have much smaller overlap with the top atomic layer due to their node in front of the surface [23]; therefore much smaller spin effects are expected than in the case of $n = 1$ states (no nodes). Yet, both image states have very similar spin splittings, as is shown below.

The energy dispersion of the image state $n = 1^-$ is displayed in the form of an $E(k_{||})$ diagram in Fig. 2. The effective vacuum levels induce a downward dispersion [21]; it is approximated by a parabola giving an effective mass $\frac{m^*}{m} = -(0.28 \pm 0.03)$ near $\overline{Y}$. The IPE intensity of the state $n = 1^+$ is observed to decrease rapidly upon deviation from $\overline{Y}$. This behavior is in accordance with the theoretically expected convergence of the state's energy towards E_V [21]; on aproaching E_V the maximum of the wave function moves away from the surface into the vacuum, resulting in a little overlap with IPE initial states.

Figure 3 presents spin-resolved IPE spectra of the $n = 1^-$ and $n = 1^+$ image states. For both states a large splitting between majority and minority peak energies of about 100 meV is clearly discernible. These spin splittings are almost an order of magnitude larger than any image-state splitting so far observed on clean surfaces [3, 6].

In order to obtain exact values for the splittings we performed a simultaneous least-squares-fit analysis of the majority and the minority spectrum, using a common parameter set for both spectra; this procedure ensures that spin-independent parameters are varied in both spectra at the same time. Each spectrum is composed of two Lorentzians (with spin-dependent energy positions and spin-independent linewidths) plus a linear background and a steplike increase of the background near E_V, convoluted by a Gaussian to account for finite experimental resolution. The background is assumed to be equal in both spectra except for an offset due to the larger minority density of states just above E_F serving as final states for inelastically scattered electrons [6]. The steplike background is described by a spin-independent parabolic function steeply increasing on approaching E_V from below [24]. The *absolute* peak positions, determined by the fit, change up to 50 meV upon varying the shape of the parabola between "soft" and steplike. Yet, the *relative* energy positions between majority and minority states are almost independent of the background form (changes < 10 meV); the best fit curves are shown as solid curves in Fig. 3. The obtained spin splittings are $\Delta E_{ex}^{1-} = 125 \pm 24$ meV for the $n = 1^-$ and $\Delta E_{ex}^{1+} = 96 \pm 30$ meV for the $n = 1^+$ state. These values are equal (within 1% of accuracy) to the exchange splittings ($\equiv \Delta E_{ex}$ at $k_{||} = \text{const}$) *at* the SBZ boundary $\overline{Y}$ since the energy is a stationary function of $k_{||}$ at $\overline{Y}$. The fact that ΔE_{ex}^{1-} is not considerably smaller than ΔE_{ex}^{1+} strongly supports the assignment of the upper state to an $n = 1$ state that has no nodes outside the crystal and hence a much larger overlap with the exchange-split band structure of the surface layer than an $n = 2$ state.

Using the known experimental resolution (FWHM = 393 meV [3,15]) and assuming a spin-independent intrinsic linewidth the fit analysis yields 185 ± 50 meV (FWHM) and an upper limit of 120 meV for the $n = 1^-$ and the $n = 1^+$ states linewidths, respectively. Thus the exchange splittings are nearly as large as the linewidths.

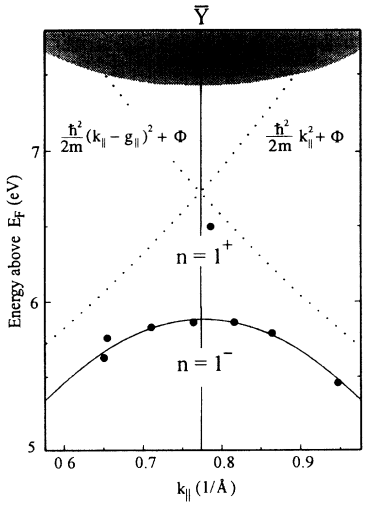

FIG. 2. Dispersion of the image-potential state $n = 1^-$. The downward dispersion is induced by the effective vacuum levels (dotted curves); $g_{||}$: reciprocal lattice vector (0,0,0,2) $2\pi/c$. The parabola (solid curve) least squares fitted to spin-integrated experimental data yields an effective mass $m^*/m = -0.28$ near $\overline{Y}$.

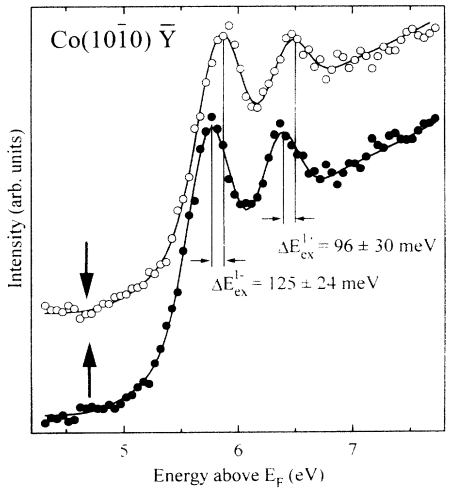

FIG. 3. Spin- and symmetry-split $n = 1$ image potential state at the surface Brillouin zone boundary $\overline{Y}$ of Co(10$\bar{1}$0). The solid curve through the data points represents the spectral description obtained by a simultaneous least-squares-fit analysis of both spin spectra. For details see text.

Therefore, electrons which are captured in these two-dimensional nearly free-electron states are highly spin polarized.

A qualitative understanding of the image-state exchange splitting is achieved in the multiple-reflection model for Shockley surface states [1, 5]. For a quantitative application of this model to the present case we assumed a spin-independent surface-barrier potential, approximated by the McRae formula [25]. The influence of the crystal is described by the two-band model [21] using the theoretical exchange splittings of the upper and lower gap boundary at $\overline{Y}$ as 0.96 eV and 0.67 eV, respectively [13]. The image plane position is chosen such that the spin-integrated energy position of both $n = 1$ states and the experimental spin splitting of the $n = 1^-$ state are matched. It is found that the spin splitting of the $n = 1^+$ state is underestimated by more than a factor of 2. The reason for this discrepancy is presumably partly inherent in the phase-model description at SBZ boundaries: It considers the upper state of the symmetry-split pair by an offset of π in the crystal phase [5, 21]. Hereby, the $n = 1^+$ state is effectively treated as a state "between" $n = 1$ (no nodes) and $n = 2$ (one node) which leads to an underestimation of the overlap of the $n = 1^+$ state with the spin-split bands of the surface layer.

On the other hand, the impossibility of describing energy positions and exchange splittings of both states within the model may indicate a possible spin dependence of the surface-barrier potential. This has been suggested for the case of Fe(110) where spin effects of the barrier are expected to influence the image-state splitting by $\approx 10\%$ [8]. Yet no experimental information is available for this surface. Furthermore, it seems impossible to unambiguously show a barrier-spin dependence in the case of the very small splittings on Ni surfaces [26]. By contrast, the much larger image-state splittings observed in the present case should allow a stringent test for possible spin effects of the surface-barrier potential.

In summary, we have identified, for the first time, a symmetry-split pair of $n = 1$ image states. Their energy separation is a measure of the effective corrugation of the surface potential a few Å in front of the crystal. Both image states are strongly exchange split by 125 meV and 96 meV, respectively, which is almost an order of magnitude larger than previously observed on clean ferromagnetic surfaces. The splittings are comparable with the intrinsic linewidths so that these two-dimensional nearly free-electron states in front of Co($10\overline{1}0$) are highly spin polarized. The large exchange splitting of these states protruding far into the vacuum renders this surface a good test case to answer the long-standing question whether or not spin effects of the barrier potential must be considered.

It is a pleasure to thank N. Memmel for stimulating discussions and J. Noffke for the band structure calculations. One of us (P.R.) gratefully acknowledges continuous support by K. Christmann. This work was supported by the Deutsche Forschungsgemeinschaft SFB 290/TPA6.

[1] P. M. Echenique and J. B. Pendry, J. Phys. C **20**, 2065 (1978).
[2] M. Donath, V. Dose, K. Ertl, and U. Kolac, Phys. Rev. B **41**, 5509 (1990).
[3] K. Starke, K. Ertl, and V. Dose, Phys. Rev. B **45**, 6154 (1992).
[4] A. Goldmann, V. Dose, and G. Borstel, Phys. Rev. B **32**, 1971 (1985).
[5] N. V. Smith, Phys. Rev. B **32**, 3549 (1985).
[6] F. Passek and M. Donath, Phys. Rev. Lett. **69**, 1101 (1992).
[7] N. Fischer, S. Schuppler, Th. Fauster, and W. Steinmann, Phys. Rev. B **42**, 9717 (1990).
[8] M. Nekovee, S. Crampin, and J. E. Inglesfield, Phys. Rev. Lett. **70**, 3099 (1993).
[9] J. Redinger, C. L. Fu, A. J. Freeman, U. König, and P. Weinberger, Phys. Rev. B **38**, 5203 (1988).
[10] F. J. Himpsel and E. D. Eastman, Phys. Rev. B **21**, 3207 (1980).
[11] H. Scheidt, M. Glöbl, V. Dose, and J. Kirschner, Phys. Rev. Lett. **51**, 1688 (1983).
[12] F. J. Himpsel, Phys. Rev. B **43**, 13 394 (1991).
[13] J. Noffke (private communication).
[14] M. Donath, M. Glöbl, B. Senftinger, and V. Dose, Solid State Commun. **60**, 237 (1986).
[15] W. Grentz, M. Tschudy, B. Reihl, and G. Kaindl, Rev. Sci. Instrum. **61**, 2528 (1990).
[16] K. Starke, K. Ertl, and V. Dose, Phys. Rev. B **46**, 9709 (1992).
[17] A detailed description of the normalization procedure can be found in Ref. [16] and in Ref. [6].
[18] Spin-resolved studies of hcp Co d bands and crystal-induced states will be published elsewhere.
[19] W. Jacob, V. Dose, U. Kolac, Th. Fauster, and A. Goldmann, Z. Phys. B **63**, 459 (1986).
[20] A. Goldmann, M. Donath, W. Altmann, and V. Dose, Phys. Rev. B **32**, 837 (1985).
[21] C. T. Chen and N. V. Smith, Phys. Rev. B **35**, 5407 (1987).
[22] V. Dose, Th. Fauster, and R. Schneider, Appl. Phys. A **40**, 203 (1986).
[23] E.g., V. Dose, Phys. Scr. **36**, 669 (1987).
[24] Compare Fig. 4 in Ref. [12].
[25] E. G. McRae, Rev. Mod. Phys. **51**, 541 (1979).
[26] In the case of Ni(111) the calculated spin dependence of the barrier reduces the image-state splitting at $\overline{\Gamma}$ by only 2 meV [M. Donath (private communication)].

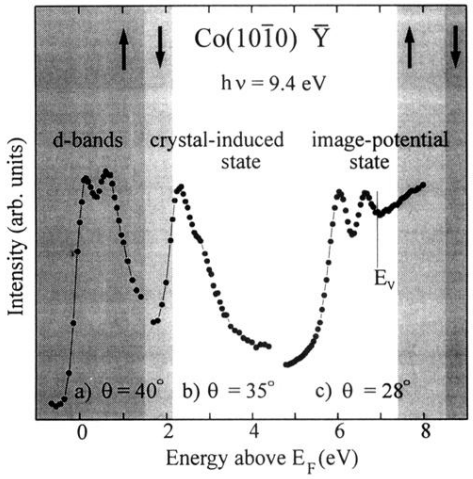

FIG. 1. Spin-integrated IPE spectra of (a) the d-band, (b) the crystal-induced, and (c) the image-potential surface states on Co(10$\bar{1}$0) near the SBZ boundary $\overline{Y}$. The spectra were taken at three different angles of electron incidence: (a) $\Theta = 40°$, (b) $\Theta = 35°$, and (c) $\Theta = 28°$ relative to the surface normal. The energy range of the spin-dependent bulk band structure (from Ref. [13]) is indicated by shaded areas. E_V denotes the effective vacuum energy at $\overline{Y}$ $E_V = \Phi + \hbar^2 k_{||}^2/2m = 6.72$ eV with $\Phi = 4.45$ eV.

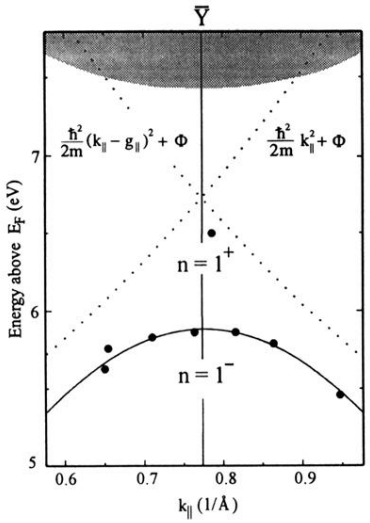

FIG. 2. Dispersion of the image-potential state $n = 1^-$. The downward dispersion is induced by the effective vacuum levels (dotted curves); $g_{||}$: reciprocal lattice vector (0,0,0,2) 2 π/c. The parabola (solid curve) least squares fitted to spin-integrated experimental data yields an effective mass $m^*/m = -0.28$ near $\overline{Y}$.